Magnetic phase diagram of $NiCl_2 \cdot 6H_2O$: The low-temperature canted-paramagnetic boundary and the bicritical point

N. F. Oliveira, Jr.

Instituto de Física, Universidade de São Paulo, C.P. 20516 São Paulo, S. P., Brazil and Francis Bitter National Magnet Laboratory, Massachusetts Institute of Technology, Cambridge, Massachusetts 02139

A. Paduan Filho, S.R. Salinas, and C.C. Becerra

Instituto de Física, Universidade de São Paulo, C.P. 20516 São Paulo, S. P., Brazil

(Received 5 July 1978)

The magnetic phase diagram of the antiferromagnetic $NiCl_2 \cdot 6H_2O$ ($T_N = 5.34$ K) was determined from dM/dH measurements down to temperatures T as low as 0.35 K, and in magnetic fields H up to 150 kG. The $T = 0$ spin-flop field and canted-paramagnetic critical field were determined as $H_{SF}(0) = 39.45 \pm 0.30$ kG and $H_c(0) = 143.9 \pm 1.5$ kG, respectively. From these values, the exchange field $H_E = 77.4 \pm 0.9$ kG and the uniaxial anisotropy field $H_A = 10.8 \pm 0.3$ kG were obtained. The corresponding single-ion parameters are $z|J|/k_B = 11.5 \pm 0.3$ K and $|D|/k_B = 1.61 \pm 0.07$ K. These values are compared with the ones obtained previously from other experiments. A careful analysis of the temperature dependence of the canted-paramagnetic critical field H_c is presented. For $T \lesssim 0.25 T_N$, the $T^{3/2}$ dependence predicted by Green's-function and spin-wave calculations is observed. For $0.3 T_N \lesssim T \lesssim 0.6 T_N$, the observed T dependence is *approximately* $T^{5/2}$, similar to the results of Rives *et al.* in $MnCl_2 \cdot 4H_2O$ and $CoCl_2 \cdot 6H_2O$ for comparable reduced temperatures. Our results suggest that temperatures above $0.3 T_N$ are too high for comparing the T dependence of H_c with spin-wave theory. Near the bicritical point ($H_b = 44.22$ kG and $T_b = 3.940$ K) the boundaries were determined with higher precision, and compared with the recent predictions based on scaling and renormalization-group theories. Colinearity between $\vec{H}$ and the easy axis was achieved to about 0.1 degrees. Least-squares fits indicated good overall agreement with the theoretical predictions for the case where the number of critical spin components is $n = 2$.

I. INTRODUCTION

The magnetic phase boundaries of low-anisotropy antiferromagnets, in the magnetic-field-temperature (H-T) plane, have been the subject of experimental[1-8] and theoretical[9-16] studies in the past years. Of special interest is the case when $\vec{H}$ is parallel to the easy axis a'. In this case and at $T = 0$, by increasing H, two transitions are observed: (i) at a field $H_{SF}(0)$, a first-order transition (the spin-flop transition) separates the longitudinally ordered antiferromagnetic (AF) phase from the perpendicularly ordered canted (C) phase, also called spin-flop phase; and (ii) by further increasing H (at $T = 0$), a second-order transition at $H_c(0)$ separates the C phase from the paramagnetic (P) phase. As T is increased, the first-order line of spin-flop transition $H_{SF}(T)$ terminates at the bicritical point (H_b, T_b), where this boundary meets both the AF-P and C-P second-order lines. The AF-P boundary extends from (H_b, T_b) to $(H = 0, T_N)$, T_N being the Néel temperature. The C-P boundary extends from $(H_c(0), T = 0)$ to (H_b, T_b).

The general features of this phase diagram have been known for a long time from the molecular-field approximation (MFA). However, some particular aspects have been studied also by more sophisticated theoretical approaches, and significant discrepancies from the expected MFA behavior have been predicted. In the present paper, measurements of the magnetic phase diagram of $NiCl_2 \cdot 6H_2O$ are presented and discussed with emphasis on two aspects for which such theoretical treatments exist: (i) the T dependence of the C-P boundary at low T;[9-12] and (ii) the behavior of the phase boundaries as they meet at the bicritical point.[13-16]

The T dependence of the C-P boundary at low T has been calculated by several authors, using different techniques and for different kinds of anisotropy. Falk[9] studied the isotropic case based on a variational method. Anderson and Callen,[10] in a comprehensive study using Green's-function techniques, included uniaxial single-ion anisotropy. The spin-wave calculations of Feder and Pytte[11] allowed also for a uniaxially anisotropic exchange. All these calculations predicted that, at low T, the C-P boundary should be given by

$$H_c(T) = H_c(0)(1 - c_1 T^{3/2} - c_2 T^{5/2}) + \cdots ,$$

and, therefore, the asymptotic dependence for $T \to 0$ should be of the form $T^{3/2}$. However, very recently, Cieplak[12] has shown that the inclusion in spin-wave calculations of either an orthorhombic single-ion anisotropy or a transversally ani-

sotropic exchange, ($J_x \neq J_y$) changes the asymptotic behavior from $T^{3/2}$ to T^2.

The experimental verification of these predictions is made difficult by the necessity of combining high H with low T. For a simple antiferromagnet with $T_N \simeq 10$ K (and $S \sim 1$), $H_c(0)$ is expected to be $\gtrsim 200$ kG.[17] $NiCl_2 \cdot 6H_2O$ presents a rare opportunity: in the present work, the combination of ^{3}He techniques with a Nb_3Sn superconductive magnet, allowed measurements of $H_c(T)$ down to $T \simeq 0.07T_N$, where $H_c \simeq 143$ kG. A $T^{3/2}$ dependence was clearly exhibited at the lowest T, but deviations from this law were shown for $T > 0.25T_N$.

The second aspect studied here, the behavior of the phase boundaries very near (H_b, T_b), was the subject of calculations by Fisher, Nelson, and Kosterlitz[13-16] (FNK) based on scaling and renormalization-group theories. According to FNK, the AF-P and the C-P boundaries should join the AF-C boundary smoothly, that is, the three boundaries should have the same tangent at (H_b, T_b). In addition the temperature dependence of the second-order lines (AF-P and C-P boundaries) should be governed by the crossover exponent which in turn depends on the anisotropy. These predictions are in dramatic contradiction with the MFA, according to which each boundary should have a different tangent at (H_b, T_b), with both AF-P and C-P boundaries being linear in H^2.

The predictions of FNK concerning the bicritical point were first fully verified in the orthorhombic antiferromagnet $GdAlO_3$.[5] Subsequent measurements in[6,7] MnF_2 and[8] Cr_2O_3 showed good qualitative agreement with theory, although quantitatively some difficulties were reported. In order to obtain data suitable for comparison with this theory, in addition to the high precision usually needed in investigations of critical phenomena, accurate parallelism between $\vec{H}$ and the easy axis (a' axis) is extremely important. In the present work such alignment was obtained to within $\sim 0.1°$. The data showed good quantitative agreement with the FNK predictions.

The phase boundaries of $NiCl_2 \cdot 6H_2O$ were determined from the H and T dependence of the differential susceptibility dM/dH. In the presence of H, the magnetic transitions are usually associated with peaks in the curves of dM/dH vs H or T, allowing an accurate determination of the phase boundary.[2-6] Short reports on some of the data of this article have been presented earlier.[18]

$NiCl_2 \cdot 6H_2O$ is a monoclinic salt whose magnetic properties have been extensively investigated. The magnetic and crystal structure determinations by Kleinberg,[19] the antiferromagnetic-resonance work of Date and Motokawa,[20] the calorimetric investigations of Johnson and Reese,[21] and the susceptibility studies of Hamburger and Friedberg[22] are of relevance to the present work. They show that $NiCl_2 \cdot 6H_2O$ is an antiferromagnet with $T_N = 5.34$ K, and with the following characteristics: (a) the exchange energy is larger than the anisotropy energy by one order of magnitude; (b) the anisotropy is of the single-ion type and possesses nearly uniaxial symmetry; and (c) the easy axis a' lies in the a-c plane at an angle of about 10° from the a axis. The antiferromagnetically ordered spin structure is shown in Fig. 1.

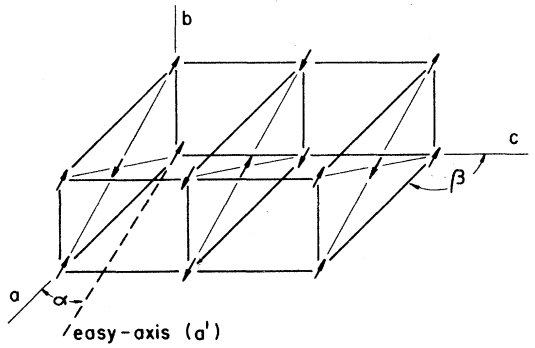

FIG. 1. Magnetic structure of $NiCl_2 \cdot 6H_2O$. The dimensions of the unit cell are: $a = 10.23$ Å, $b = 7.05$ Å, $2c = 13.14$ Å, and $\beta = 122°10'$. The easy axis, a', lies in the a-c plane and makes an angle $\alpha \simeq 10°$ with the a axis.

II. THEORETICAL RESULTS

A. Low-temperature phase boundaries

Consider the Hamiltonian

$$\mathcal{H} = -J \sum_{\langle \alpha,\beta \rangle} \vec{S}_\alpha \cdot \vec{S}_\beta - D \sum_\alpha S_{\alpha z}^2 + \sum_\beta S_{\beta z}^2 \; - g\mu_B H \left(\sum_\alpha S_{\alpha z} + \sum_\beta S_{\beta z} \right), \tag{1}$$

neighbor pairs, and α and β label the lattice sites in the α and β sublattices, respectively. The J term represents the isotropic Heisenberg exchange interaction, the D term gives the single-ion uniaxial anisotropy, and the last term is the usual Zeeman term.

1. C-P boundary at low T

With $\vec{H}$ parallel to a', both MFA and spin-wave calculations predict the same value for the C-P critical field $H_c(0)$ at $T = 0$, namely,

$$H_c(0) = 2H_E - H_A = 2z\,|J|/g\mu_B - |D|/g\mu_B, \tag{2}$$

where $H_E = z|J|/g\mu_B$ is the exchange field, $H_A = |D|/g\mu_B$ is the anisotropy field, and z is the number of nearest neighbors.

The Green's-function analysis of Anderson and Callen[10] applied to the Hamiltonian of Eq. (1), with $S=1$, gives the following expression for the T dependence of H_c in the low-T region

$$H_c(T) = H_c(0)\{1 - 2b_0\tau^{3/2} - [H_E/H_c(0)]\tfrac{4}{3}b_1\tau^{5/2}\}, \tag{3}$$

where $\tau = k_BT/g\mu_BH_E$, and b_0 and b_1 are constants that depend on the lattice structure. Values for these constants have been obtained for two different lattices[10]: for simple cubic (sc), $b_0 = 0.8617\ldots$ and $b_1 = 0.4981\ldots$; for bcc, $b_0 = 0.6634\ldots$ and $b_1 = 0.3834\ldots$. The spin-wave result of Feder and Pytte[11] for a sc lattice, and the variational calculation of Falk[9] include only the $T^{3/2}$ term, and both agree with Eq. (3).

2. AF-C transition (spin flop)

The AF-C transition is a first-order transition, but hysteresis is usually not observed.[23] Spin-wave theory gives expressions for the stability limits of the AF phase (with increasing H), and the stability limit of the C phase (with decreasing H).[11] The experimentally observed transitions occur at the field value $H_{SF}(T)$ at which the free-energies of both phases are equal.[23] From MFA, the value $H_{SF}(0)$, for $T=0$, is given by

$$H_{SF}(0) = [H_A(2H_E - H_A)]^{1/2}. \tag{4}$$

3. H perpendicular to a'

For $\vec{H}$ perpendicular to a', the phase diagram is just a single boundary that separates the ordered phase from the P phase. The MFA expression for the critical field at $T=0$ is

$$H_c^{\perp}(0) = 2H_E + H_A. \tag{5}$$

B. Bicritical point

The FNK calculations[13-16] predict that the AF-P and C-P critical lines should meet the spin-flop line tangentially at (H_b, T_b), with a curvature characterized by the crossover exponent $\phi > 1$. Near the bicritical point, the scaling hypothesis suggests the introduction of the optimum linear scaling fields given by

$$\tilde{t} = t + qg \quad \text{and} \quad \tilde{g} = g - pt, \tag{6}$$

where $t = (T - T_b)/T_b$ and $g = H^2 - H_b^2$. The slope p should be given by

$$p = \frac{1}{T_b}\left(\frac{dH_{SF}^2(T)}{dT}\right)_{T=T_b}, \tag{7}$$

so that the $\tilde{g}=0$ axis corresponds to the limiting tangent to the spin-flop line at the bicritical point. Fisher[14] gives the following expression for the thermal axis slope q,

$$q \simeq -\frac{n+2}{3n}\frac{1}{T_b}\left(\frac{dT_c^{\parallel}}{dH^2}\right)_{H=0}, \tag{8}$$

where n is the total number of spin components exhibiting divergent bicritical fluctuations. For a perfectly uniaxial system $n=3$, but if some degree of anisotropy is present in the plane perpendicular to the easy-axis, one has $n=2$. $T_c^{\parallel}$ in Eq. (9) represents the AF-P boundary.

The critical lines near the bicritical point are given by

$$\tilde{g}_c = \omega_{\perp}\tilde{t}^{\phi} \quad \text{and} \quad \tilde{g}_c = -\omega_{\parallel}\tilde{t}^{\phi}, \tag{9}$$

for the canted and antiferromagnetic boundaries respectively. Series expansions[24] yield the values $\phi(n=3) = 1.25$ and $\phi(n=2) = 1.18$ for the crossover exponent. The ratio $Q(n) = \omega_{\perp}/\omega_{\parallel}$ has also a universal character. Renormalization-group arguments show that $Q(2)=1$, whereas $Q(3) \cong 2.51$.

III. EXPERIMENTAL DETAILS

Single crystals of $NiCl_2 \cdot 6H_2O$ were grown from reagent grade salt by evaporation from aqueous solution at about 30 °C. The crystal axes could be identified from the growth habit described by Groth.[25] The samples used were elongated in the a direction and had roughly the shape of a parallelepiped. The dimensions of a typical sample were $0.7 \times 0.2 \times 0.2$ cm. To avoid deliquescence, the crystals were maintained in pure clock oil, and received a heavy coat of silicon grease before being mounted in the sample holder. To avoid storage for long periods of time, new crystals were used whenever a new set of runs was started.

The variable temperature cryostat used was similar to the one described by Oliveira and Quadros.[26] The cryostat consisted essentially of a small double wall variable temperature chamber, insulated by vacuum from a surrounding thermal bath. Inside the chamber, well controlled amounts of either ^{3}He or ^{4}He could be liquefied and the temperature of the liquid ^{3}He or ^{4}He could be controlled by the vapor pressure. During the measurements, the volume of liquid in which the sample was immersed was never larger than 5 cm^3 and the height of the column above the sample never exceeded 2 cm. In this way, the problem of temperature corrections due to the height of the liquid column was avoided.[27] The

presence of the outside bath provided improved stability to the sample bath. In the ^{4}He range, the variable T chamber was immersed directly in the 4.2-K bath of the superconducting coil which produced H. For the ^{3}He range, an insert dewar had to be placed inside the bore of the magnet so that the variable T chamber could be surrounded by a 1.2-K ^{4}He bath. The temperature was determined by measuring the vapor pressure using a conventional Hg-oil manometer and a "Baratron" gauge.[28] A few points were taken just above 4.2 K. For those, T was obtained from a glass capacitance thermometer[29] calibrated in the ^{4}He range. The overall accuracy in the measurement of T was always better than 0.01 K. For the measurements near (H_b, T_b) (3.8 to 4.1 K) special care was taken to achieve a precision better than 0.002 K.

The dM/dH was measured with an ac mutual inductance bridge similar to that described by Maxwell.[30] The secondary coils (pickup coils) were wound on an epoxy-resin spool and placed inside the sample chamber. A cylindrical capsule of the same epoxy resin, made to fit snugly the bore of the pickup coils (0.6 cm), housed the sample holder. The set sample-holder–secondary-coils was made as small as possible to minimize spurious pickup coming from the external magnetic field. The primary measuring coil was placed in the outside bath surrounding the sample chamber. Except when otherwise indicated, the measuring frequency was 155 Hz and the modulation field ~3 Oe. The external field was produced by two different superconducting magnets. For the highest fields (up to 150 kOe) a Nb_3Sn magnet with homogeneity better than 0.1% in 1 cm was used. With this magnet, the field value was obtained from a magneto-resistive probe calibrated with an overall accuracy of better than 1%, but with a resolution for measuring field variations of about 100 Oe. Below 75 kOe a NbTi magnet was preferred because of its better homogeneity (0.01% in 2.5 cm), the practical absence of trapped flux (less than 20 Oe) and the ease of operation. For this magnet, the proportionality between field and current was calibrated to within 0.5% and the resolution for field variations was ~30 Oe.

To achieve the necessary degree of alignment between $\vec{H}$ and the sample easy axis, a suspension system was devised which permitted small changes in the direction of the axis of the superconducting coil. Figure 2 shows schematically the magnet suspension. The coil was suspended by three stainless steel posts whose lengths could be varied by fine thread screws at the top flange of the cryostat. These posts were connected by movable joints to a ring of phenolic material which was rigidly tied to the coil at its mid plane. With this simple construction it was possible to tilt the coil axis by approximately 3° in any direction, with a resolution better than 0.05°. The variable temperature chamber was considerably narrower than the bore of the magnet, and was held fixed inside the bore by a styrofoam spacer at the mid plane of the coil (see Fig. 2).

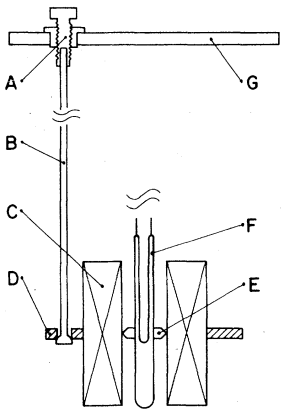

FIG. 2. Schematic view of the suspension of the NbTi superconducting magnet. *A*: adjusting screw; *B*: stainless steel post; *C*: coil; *D*: phenolic ring rigidly tied to the coil; *E*: styrofoam spacer; *F*: variable temperature chamber; *G*: top flange of the cryostat.

IV. RESULTS AND DISCUSSION

Most of the transition fields were obtained from continuous curves of dM/dH (output of the mutual inductance bridge) vs H at constant T. At the spin-flop transition, the magnetization is discontinuous, and the differential susceptibility with respect to the internal field becomes infinite. The measured susceptibility (with respect to the applied field) shows a large (but finite) sharp peak whose width and height are dependent on the demagnetization factor of the sample and the size of the magnetization jump.[2,3] At the C-P transitions, a λ peak is observed, due to spin fluctuation effects. These peaks become less conspicuous as T increases (and the boundaries become steeper in the H-T plot).

Near the bicritical point, each of the boundaries were marked by a dM/dH peak whose shape and/or size was peculiar to that boundary. With increasing T, the spin-flop peaks diminished rapidly as T approached T_b and then changed smoothly into smaller, but still sharp, AF-P λ-type peaks. The C-P peaks in dM/dH vs H, however, were broad and almost imperceptible. A precise location of this C-P boundary was possible only from plots of dM/dH vs T at constant H, where a well defined small λ peak could be observed. A comparison between the two methods of determining the

TABLE I. Critical fields for $NiCl_2 \cdot 6H_2O$ (uncorrected for sample demagnetization), obtained in the present work. Except where otherwise indicated, points were obtained by sweeping H at constant T, and with $\vec{H}$ parallel to the easy axis. Data are presented in blocks corresponding to different runs.

Antiferro–para		Antiferro–canted		Canted–para	
T (K)	H_c (kOe)	T (K)	H (kOe)	T (K)	H_c (kOe)
4.82	30.00	0.350	39.47	0.380	142.7
4.75	31.80	0.400	39.45	0.400	142.6
4.70	33.00	0.450	39.45	0.450	142.5
4.40	38.80	0.500	39.45	0.500	142.2
		0.600	39.47	0.550	141.9
4.132	42.24	0.700	39.49	0.600	141.6
4.107	42.53	0.800	39.51	0.650	141.3
4.087	42.76	0.900	39.53	0.700	141.0
4.066	43.03	1.000	39.55	0.750	140.6
4.042	43.29	1.100	39.60	0.800	140.3
4.018	43.54 [a]	1.200	39.67	0.850	140.0
3.995	43.77 [a]	1.300	39.69	0.955	139.3
3.971	43.99 [a]	1.400	39.86	1.004	138.9
3.949	44.19 [a]			1.053	138.5
		1.060	39.58	1.103	138.1
4.022	43.49	1.120	39.61	1.153	137.8
4.011	43.61 [a]	1.310	39.76	1.252	136.9
3.993	43.79 [a]	1.570	39.94	1.301	136.4
3.980	43.92 [a]	1.850	40.24		
3.966	44.05 [a]	2.080	40.47	1.252	136.9
3.952	44.16 [a]	2.380	41.05	1.300	136.5
3.943	44.20 [a]	2.720	41.72	1.400	135.6
		3.000	42.20	1.500	134.6
For $\vec{H} \parallel \hat{b}$		3.090	42.33	1.600	133.6
2.821	138.7	3.670	43.65	1.700	132.6
2.680	141.3			1.900	130.3
3.027	135.2	3.883	44.11	2.000	129.1
3.233	131.3	3.898	44.13	2.100	127.8
3.436	127.0	3.906	44.15		
3.661	122.0	3.913	44.16	1.638	133.5
3.866	116.5	3.920	44.18	1.780	131.8
4.150	108.4	3.932	44.20	2.019	129.0
				2.169	127.0
		3.645	43.60	2.574	121.0
		3.679	43.67	2.859	115.2
		3.731	43.78	3.164	107.9
		3.786	43.90		
		3.828	43.99	3.943	44.27 [a, b]
		3.858	44.05	3.945	44.31 [a, b]
		3.917	44.17	3.949	44.33 [a, b]
		3.924	44.18	3.950	44.35 [a, b]
		3.930	44.19	3.953	44.41 [a, b]
		3.937	44.21	3.957	44.52 [a, b]
				3.961	44.64 [a, b]
				3.967	44.79 [a, b]
				3.973	45.08 [b]
				3.959	45.46 [b]
				3.983	46.30 [b]
				3.996	47.00 [b]
				4.018	49.00 [b]
				4.042	53.00 [b]
				3.872	80.18 [b]
				3.596	94.98 [b]
				3.576	96.19

[a] Points used for the fits with Eqs. (9).

[b] Points obtained by varying temperature at constant field.

phase boundary, i.e., from plots of dM/dH vs H and from plots of dM/dH vs T, could be made at $H \simeq 95$ kOe and $T \simeq 3.6$ K where the C-P boundary could be observed equally well by both methods. The results agreed within the experimental resolution.

For all points obtained from plots of dM/dH vs H at constant T, the observed rounding of the susceptibility peaks was small enough so that the related uncertainty in locating the critical field was within our experimental resolution for measuring H. For the transitions located from curves of dM/dH vs T at constant H, the total uncertainty in locating the critical temperatures was estimated to be ±2.5 mK.

The critical fields determined in the present work are tabulated in Table I. The values given there are those for the applied field. Such values differ from the internal fields that appear in the theoretical equations presented in Sec. II by the demagnetizing field of the samples H_d. For the present measurements, H_d can be expressed as a small percentage correction to the applied field H, and for $\vec{H}$ parallel to a', H_d amounts to just 0.1% of H. This estimate was made from the measured susceptibility and the demagnetization factor obtained from the height of the dM/dH peaks at the spin-flop transition. This demagnetization factor obtained from the spin-flop peaks agrees with the value calculated for a prolate elipsoid with a dimensional ratio equal to that of the samples used.[31] Such a value of H_d is negligibly small when compared to the uncertainty in field calibration. In fact, H_d is comparable to the ultimate experimental resolution in the measurement of H. Thus, to within the accuracy and precision of the present work, the values of H presented in Table I can be regarded also as internal fields for the samples used. All the best fits that will be described later were made using values of H given in Table I.

Figure 3 shows an overall picture of the data, including the points obtained from the specific heat measurements of Johnson and Reese.[21] It also shows data for $\vec{H}$ oriented along the b axis, which is perpendicular to a'.

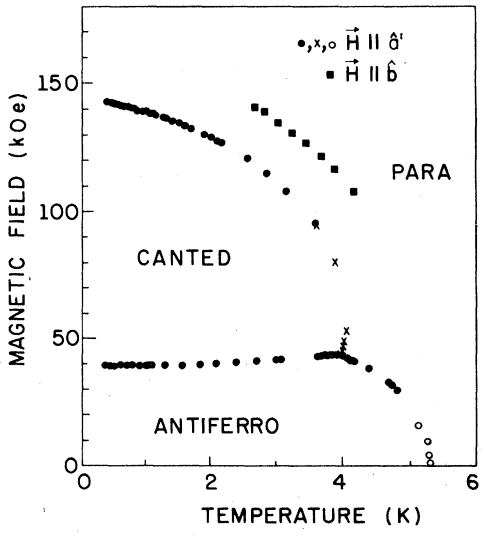

FIG. 3. Experimentally determined magnetic phase diagram of $NiCl_2 \cdot 6H_2O$ for $\vec{H}$ parallel to the easy axis a', and for $\vec{H}$ parallel to the b axis. The open circles represent points from the calorimetric work of Johnson and Reese (Ref. 21). All other points are from the present work. Crosses represent points obtained from plots of (dM/dH) vs T at constant H. All other points of the present work were obtained from plots of dM/dH vs H at constant T.

A. Exchange and anisotropy parameters

The exchange and anisotropy parameters could be obtained from extrapolations to $T = 0$ of the spin-flop and C-P boundaries. The extrapolation method is described in the following sections of this article. The values obtained were $H_{SF}(0) = 39.45 \pm 0.30$ kG and $H_c(0) = 143.9 \pm 1.5$ kG. The quoted uncertainties are largely due to the experimental uncertainty in the calibration of the magnets. Using these values, the phenomenological exchange and anisotropy fields could be calculated from Eqs. (2) and (4) as $H_E = 77.4 \pm 0.9$ kG and $H_A = 10.8 \pm 0.3$ kG. With $g = 2.22 \pm 0.01$,[22] the corresponding exchange and anisotropy parameters of the single-ion Hamiltonian are $z|J|/k_B = 11.5 \pm 0.3$ K and $|D|/k_B = 1.61 \pm 0.07$ K.

Table II compares our values with results obtained previously, using different techniques. Our exchange field is 10% lower than the two other reported values. Date and Motokawa[20] derived H_E from their antiferromagnetic resonance data combined with an extrapolation to $T = 0$ of the perpendicular susceptibility measured by Haseda *et al.*[32] The value of Hamburger and Friedberg[22] was also obtained using $\chi_{\perp}(0)$, extrapolated from their own data. For $z|J|/k_B$ the latter authors quote two values. The first (12.6 K) corresponds to the value of H_E obtained from low-T data. The second (12.0 ± 0.8 K) was obtained directly from the best-fit of the paramagnetic susceptibility data versus T. This last one is in better agreement with ours. This same paramagnetic data, analyzed by Kimura[33] in a pair model approximation and assuming first and second neighbor interactions, yielded a total exchange parameter 10% lower than ours. Finally, the value ob-

TABLE II. Exchange and anistropy parameters.

Authors	H_E (kG)	$z\|J\|/k_B$ (K)	H_A (kG)	$\|D\|/k_B$ (K)	E/k_B (K)
Present	77.4 ± 0.9	11.5 ± 0.3	10.8 ± 0.3	1.61 ± 0.07	
Date and Motokawa (Ref. 20)	86		9.5 ± 0.5 [a] 12.5 ± 0.5	1.7	0.2
Hamburger and Friedberg (Ref. 22)	85	12.6 [a] 12.0 ± 0.8	10	1.5 ± 0.5	0.26 ± 0.40
Kimura (Ref. 33)		10.6		1.8 ± 0.1	0.03 ± 0.01
Iwashita and Uryu (Ref. 34)		11.7		1.00 ± 0.02	0.05 ± 0.02

[a] The two values of $z|J|/k_B$ reported by Hamburger and Friedberg (Ref. 22) correspond to two derivations of the same parameter using different data. The two values of H_A quoted by Date and Motokawa (Ref. 20) correspond to the two orthorhombic fields H_{A1} and H_{A2}.

tained by Iwashita and Uryu[34] in their spin-wave analysis of low-T susceptibility and specific heat data is in good agreement with our value. We note that, the previously reported exchange parameters rely either on an extrapolated value for $\chi_\perp(0)$ with a relatively large uncertainty, or on best fits that yield results very much dependent on the model assumed. We believe that values for $H_c(0)$ and $H_{SF}(0)$ provide a more direct and accurate way of evaluating these parameters.

Considering the anisotropy, all the above mentioned authors have included in their analyses a parameter to allow for a component of orthorhombic symmetry. Date and Motokawa[20] used two orthorhombic mean fields, H_{A1} and H_{A2}, instead of a single uniaxial field, while the other authors included the term $-E(S_y^2 - S_x^2)$ in the single-ion spin Hamiltonian. The resulting values of such parameters indicated in all cases that the orthorhombic component is small compared to the axial anisotropy. The main effect of this orthorhombic component on the phase diagram at low T, should be a slight dependence of the critical fields on the direction of $\vec{H}$, when $\vec{H}$ is rotated in a plane perpendicular to a'. We have not attempted to detect this dependence, and consequently H_E and H_A were obtained in terms of a uniaxial model. Our uniaxial parameters are in good agreement with all other reported values, except for those of Iwashita and Uryu.[34] In Fig. 3, points for $\vec{H} \| \hat{b}$, are representative of the perpendicular boundary. They appear to be consistent with the molecular field value of the $T = 0$ critical field for the perpendicular boundary, given by Eq. (5): $H_c^\perp(0) = 165.5 \pm 2$ kG.

B. Low-temperature boundaries

1. C-P boundary

The theoretical calculations of Anderson and Callen[10] and of Feder and Pytte[11] predict a $T^{3/2}$ dependence for the critical fields at $T \ll T_N$. Indeed, our earlier report on $NiCl_2 \cdot 6H_2O$ shows this dependence.[18] However, Rives and Benedict[3] and Rives and Bathia[4] have indicated a $T^{5/2}$ dependence from their measurements on $MnCl_2 \cdot 4H_2O$ and $CoCl_2 \cdot 6H_2O$, respectively. Very recently, Cieplak[12] has proposed that the inclusion in spin-wave calculations of either an orthorhombic single-ion anisotropy, or a transversally anisotropic exchange ($J_x \neq J_y$), should lead to a T^2 dependence, and that these additional terms should be valid for $MnCl_2 \cdot 4H_2O$ and $CoCl_2 \cdot 6H_2O$, respectively. For $NiCl_2 \cdot 6H_2O$, Table II shows that the anisotropy contains a small component of orthorhombic symmetry. The question then arises as to whether our experimental data are precise enough to actually distinguish between the $T^{3/2}$, T^2, or $T^{5/2}$ dependences. Furthermore, since the theory is valid only for $T \ll T_N$, there is also the question of what is the upper limit of T/T_N to observe the asymptotic dependence.

To check on these points, we have performed computer least-squares fits of the C-P critical fields to the equation

$$H_c(T) = H_c(0) - AT^\alpha, \tag{10}$$

adjusting simultaneously $H_c(0)$, A, and α. Such fits were made using several different sets of experimental points covering different temperature intervals. For each fit we have calculated the variance $\sigma^2 = (N-3)^{-1} \sum_i \delta H_{c,i}^2$ (N being the number of points fitted), and also the standard deviation for the parameters α and $H_c(0)$.[35]

From the result of these fits, two main conclusions could be drawn. First that, within the precision of the present measurements, the $T^{3/2}$ dependence is unquestionably observed for the lowest temperature points $0.38 \leq T \leq 1.3$ K (i.e., $0.07 \leq T \leq 0.24 T_N$). Second, at temperatures above 1.3 K, the critical fields decrease with faster

TABLE III. Results of least-squares fits of the canted-paramagnetic critical field H_C to the equation $H_C(T) = H_C(0) - AT^{\alpha}$, with $H_C(0)$, A, and α as ajustable parameters. Each fit includes N points from the lowest temperature T_i to the highest temperature T_f. The quoted uncertainties correspond to one standard deviation for the parameter. The values of σ correspond to the square root of the variance. $T_N = 5.34$ K is the Néel temperature.

T_i/T_N	T_f/T_N	N	α	A (kOe/K$^{\alpha}$)	$H_C(0)$ (kOe)	σ (kOe)
0.071	0.244	18[a]	1.53 ± 0.045	4.94	143.86 ± 0.10	0.05
0.188	0.593	20	2.19 ± 0.055	2.65	141.27 ± 0.28	0.27
0.243	0.593	15	2.34 ± 0.08	2.15	140.20 ± 0.43	0.24
0.300	0.593	12	2.50 ± 0.10	1.75	139.20 ± 0.58	0.23
0.307	0.593	7[a]	2.57 ± 0.15	1.61	139.0 ± 0.8	0.25

[a] All points from a single run.

rates and, therefore, fits to Eq. (10) including points well above 1.3 K lead to values of α larger than $\frac{3}{2}$.

In support to the above statements, Table III shows results of representative fits. The first result is for the fit of 18 points in the temperature interval starting at $T_i = 0.380$ K ($T_i/T_N = 0.071$), which is our lowest temperature point, and ending at $T_f = 1.301$ K ($T_f/T_N = 0.244$). All these points were measured in a single run. The best value for α is $\alpha = 1.53 \pm 0.045$, the uncertainty corresponding to one standard deviation for α. Note that the value $\sigma = 0.05$ kOe for this fit is equivalent to one half of the field-measuring resolution, indicating that this resolution was the main cause of the deviations between the experimental points and the best fit. Figure 4 which shows H_c vs $T^{3/2}$ illustrates the good quality of this fit.

The next four lines in Table III show results of fits over several temperature intervals, all with the same maximum (final) temperature $T_f = 3.164$ K ($T_f/T_N = 0.593$), but with different minimum (initial) temperatures T_i. For these fits, the following points should be noted: (i) the higher the value of T_i, the higher the value of the resulting best α; (ii) all values of α are larger than two, and, in particular, for the fit starting at $T_i = 1.600$ K ($T_i/T_N = 0.300$), $\alpha = 2.50 \pm 0.10$; and (iii) the value of σ for all these four fits are larger than twice the value of our field-measuring resolution, indicating that for these temperature intervals, a close fit with Eq. (10) cannot be obtained.

These results can provide an explanation for the $T^{5/2}$ dependence found by Rives and collaborators for the low-T C-P critical fields in $MnCl_2 \cdot 4H_2O$,[3] and $CoCl_2 \cdot 6H_2O$.[4] In both cases, the fits started at $T_i \simeq 0.25T_N$. According to Table III, our data would also show a T dependence close to $T^{5/2}$ if only points above $0.25T_N$ were fitted. It appears, then, that the data of Rives *et al.* were not taken at sufficiently low temperatures to exhibit the asymptotic low-T behavior predicted by spin-wave calculations.

Anderson and Callen[10] have extended their calculations up to the next term in the series

$$H_c(T) = H_c(0) + A'T^{3/2} + BT^{5/2}. \quad (11)$$

The coefficient B is negative, as is A' [see Eq. (3)], and they both depend on the lattice structure through the numerical factors b_0 and b_1. However, since $b_0/b_1 = 1.73$ for both sc and bcc, it seems reasonable to assume that the ratio $A'/B = (\frac{3}{2})(b_0/b_1)[g\mu_B H_c(0)/k_B]$ is insensitive to the lattice structure. Such an assumption is necessary here because there is no calculation of b_0 (or b_1) for the monoclinic lattice of $NiCl_2 \cdot 6H_2O$. Using this assumption, $g = 2.22$ (see Ref. 22) and $H_c(0) = 1.44 \times 10^5$ G (see Table III), the ratio A'/B is 55.7.

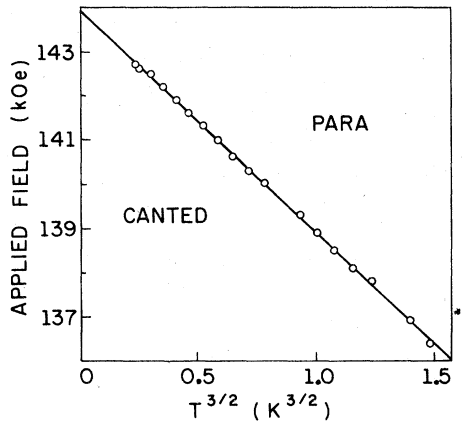

FIG. 4. Canted-paramagnetic boundary for $T \lesssim 1.3$ K, plotted vs $T^{3/2}$. Solid line represents the best fit to Eq. (10), namely $H_c(T) = 143.86 - 4.94T^{1.53}$ (H measured in kOe and T in K.

As a consequence, the predicted contribution of the $T^{5/2}$ term of Eq. (11) is smaller than the experimental resolution of our points for $T \lesssim 1$ K. This is consistent with the fact that an excellent fit was obtained with Eq. (10) (without the $T^{5/2}$ term) for the points below 1.3 K, with $\alpha \simeq \frac{3}{2}$.

To include a correction for the $T^{5/2}$ term, we have performed a least-squares fit of the data for $T \leq 1.301$ K with Eq. (11), imposing on B the restrictions of sign and ratio to A', and, therefore, adjusting $H_c(0)$ and A'. The resultant best curve was $H_c(T) = 143.90 - 4.90T^{3/2} - 0.088T^{5/2}$ (H in kG and T in K), and the quality of this fit was quite comparable to the quality of the fit of the same data with Eq. (10) (results in first row of Table III). The value $H_c(0) = 143.90$ kG was used to evaluate the exchange and anisotropy parameters. The value $A' = -4.90$ kG/K$^{3/2}$, when compared to Anderson and Callen's prediction [see Eq. (3)], leads to $b_0 = 0.668$ which is quite consistent with the two calculated values ($b_0 = 0.8617...$ and $b_0 = 0.6634...$ for sc and bcc lattices, respectively).

We have attempted, also, to fit the data up to temperatures above 1.3 K with Eq. (11). For these fits, if the theoretical restrictions of sign and ratio on the coefficients A' and B were maintained, a close fit could be obtained only up to temperatures of about 1.5 K, and the quality of the fit deteriorated rather fast as points for $T > 1.5$ K were included. On the other hand, by treating A' and B as independent adjustable parameters, a reasonable fit could be obtained up to temperatures as high as $T \simeq 3$ K, but resulting in a ratio A'/B one order of magnitude smaller than the predicted value.

2. AF-C (spin-flop) boundary

The transition from the AF phase to the C phase is a first order transition, provided that the angle between $\vec{H}$ and a' is smaller than a critical angle $\psi(T)$. $\psi(T)$ is maximum for $T = 0$ and decreases almost linearly as T increases, vanishing at $T = T_b$.[2] Mean-field theory gives $\psi(0) = H_A/2H_E$ rad,[36-37] which for $NiCl_2 \cdot 6H_2O$ amounts to $\psi(0) = 4°$. For our lowest temperature points (in the liquid-^{3}He range), an alignment better than 2° between $\vec{H}$ and a' was obtained by properly designing a sample holder and taking advantage of the known morphology of the crystal.[25] For the points in the liquid-^{4}He range, the alignment could be greatly improved by adjusting the orientation of the NbTi magnet (this procedure is described later). No discontinuity was noticed between the sets of data taken in the ^{3}He and ^{4}He range. Thus, through practically the whole temperature interval of the AF-C boundary, the alignment of $\vec{H}$ was good enough to ensure the observation of a true first order spin-flop transition.

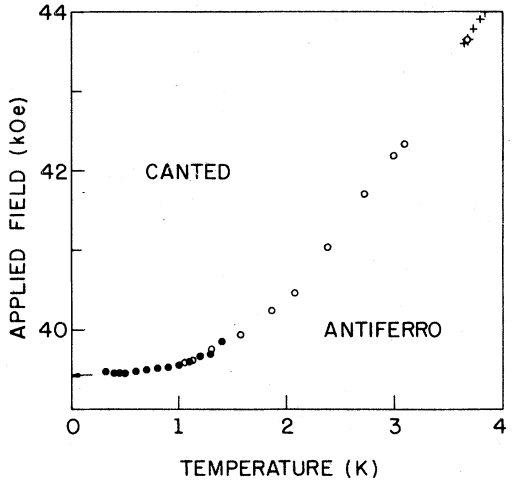

FIG. 5. Low-temperature antiferro-canted critical fields. Different symbols refer to different runs.

Figure 5 shows the temperature dependence of the measured spin-flop field $H_{SF}(T)$. These fields were determined from the maximum of the large and narrow peaks observed in curves of dM/dH vs H at constant T. For each temperature two curves were taken, one with H increasing, and another with H decreasing. The values of $H_{SF}(T)$ obtained from both always agreed within the experimental resolution.

Figure 5 shows a slow monotonic increase of $H_{SF}(T)$ with increasing T. The value $H_{SF}(0) = 39.45$ kG, used in the evaluation of the exchange and anisotropy parameters, was obtained by a smooth extrapolation of $H_{SF}(T)$ to $T = 0$.

C. Bicritical point

In the vicinity of the bicritical point, it was necessary to exercise special care to obtain higher-precision data, suitable for comparison with the theoretical predictions. Of major importance is the alignment between $\vec{H}$ and a', and a discussion of this point can be found in Ref. (5). As mentioned before, our NbTi magnet allowed fine adjustments of the orientation of $\vec{H}$ relative to the sample axes. In the present experiments, a preliminary alignment (better than ~2 degrees) was provided by the sample holder. Data taken at this preliminary alignment were sufficient to locate T_b approximately. Then, by maintaining T slightly lower than T_b, and sweeping H, a large peak was observed in dM/dH near H_b, even when

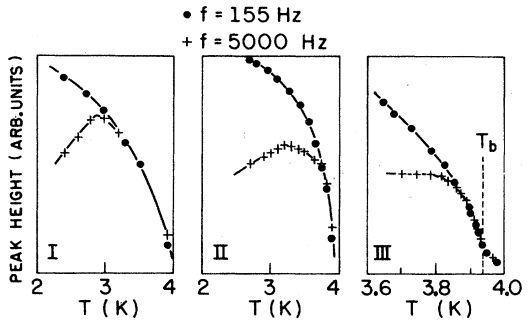

FIG. 6. Checks on the adjustments of the colinearity between field and easy axis, according to the method described in Ref. 2. At temperatures where the height of of the spin-flop peak (in dM/dH) is frequency dependent, the transition is of first order. Frames I, II, and III demonstrate the progress in the adjustment. Note the different temperature scale of frame III.

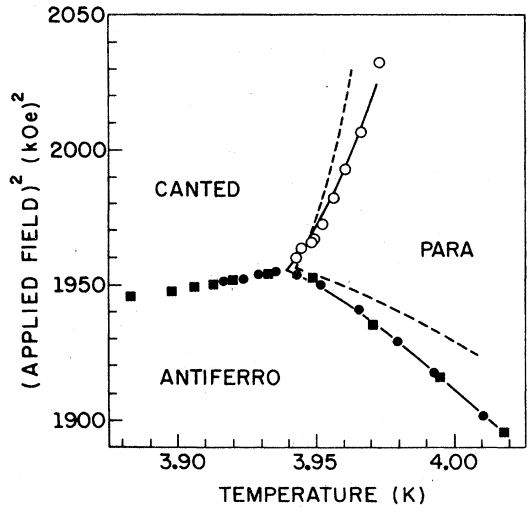

FIG. 7. Phase boundaries near the bicritical point. Different symbols represent data from different runs. The solid and dashed lines are the best fits with Eqs. (9) when only T_b and $\omega_\perp$ were adjusted. The solid line is the best fit for $n=2$, and the dashed line is the best fit for $n=3$.

the alignment was not good enough for a first-order spin-flop transition. The height of this dM/dH peak increased rapidly as the alignment was improved, and this indication was used to make the fine adjustments.

After a set of adjustments was made, the quality of the alignment could be checked by a method discussed in detail by Blazey *et al.*[2] This method consists in examining the temperature dependence of the height of the spin-flop peaks (obtained from curves of dM/dH vs H) for different modulation frequencies. Figure 6 shows the checks on the adjustment procedure for one of the experimental runs. At temperatures where a first order transition occurs, the peak height depends on the modulation frequency. In Fig. 6 I, the curves for 155 Hz and 5 000 Hz are clearly split only below $T=3$ K, indicating that only below $T=3$ K a first order transition occurs. A better alignment causes this split to occur at a temperature closer to T_b. Figure 6 II shows the improvement after some adjustment, and Fig. 6 III shows that after the final adjustment the split begins close to $T=3.85$ K. An estimate of the remaining misalignment can be made after T_b is finally determined, by assuming that the angle within which the first-order transition is observed $\psi(T)$ decreases linearly from $\psi(0)=4°$ to $\psi(T_b)=0$. For the final adjustment (Fig. 6 III), and using $T_b=3.94$ K, the actual misalignment should be $\simeq 0.1°$.[38]

Figure 7 shows the data in an H^2 scale. Two distinctive qualitative features of the FNK theory are evident in the data, in contrast with the MFA predictions. First, the critical temperatures for the C-P boundary, $T_c^\perp$, *increase* with increasing H, near H_b. According to FNK, $T_c^\perp$ should first increase with H, starting at H_b, turn around at higher H, and then, decrease to zero. MFA predicts that $T_c^\perp$ should decrease monotonically from T_b to zero. Second, both $T_c^\perp$ and $T_c^\parallel$ (the AF-P boundary) are not linear in H^2. FNK predicts that $T_c^\perp(H^2)$ and $T_c^\parallel(H^2)$ should present a curvature characteristic of the crossover between the critical regimes in the AF and C phases. MFA predicts that $T_c^\perp$ and $T_c^\parallel$ should be both linear in H^2.

In order to compare the data quantitatively with the FNK theory, the experimental points of the AF-P and C-P boundaries were fitted simultaneously with Eqs. (9). Least squares fits were performed using a computer program able to adjust simultaneously several parameters. In Eqs. (6)–(9) up to seven parameters can be made adjustable: T_b, H_b, $(dH_{SF}^2/dT)_b$, q, $\omega_\perp$, $\omega_\parallel$, and ϕ. T_b is the temperature at which the three boundaries join. In principle, one should expect to determine T_b rather accurately, directly from plots of dM/dH vs H at constant T. At T_b the sharp spin-flop peak should split into two. In our data, however, we were not able to locate precisely this splitting because the C-P transitions near (H_b, T_b) were broad and barely perceptible. In fact, as mentioned earlier, a precise determination of this boundary was possible only from plots of dM/dH vs T at constant H. A detailed plot of the experimental boundary points, as shown in Fig. 7, allowed an *a priori* location of T_b to within ±5 mK. Nevertheless, because small variations of T_b can

cause large relative variations in $\tilde{t}_i$, it was preferred to maintain T_b as an adjustable parameter in all fits performed. On the other hand, the value of $(dH_{SF}^2/dT)_b$ could be determined rather accurately by fitting the points of the spin-flop boundary for $T \geq 3.645$ K to a second degree polynomial. This same polynomial fit could give the value of H_b, after T_b had been determined. Checks have shown that the best fits to Eqs. (9) were generally quite insensitive to variations of the value of $(dH_{SF}^2/dT)_b$, and for this reason it was held constant at its determined value $(dH_{SF}^2/dT)_b = 175$ kG^2/K, in all fits performed.

The slope of the thermal axis q is related to the AF-P boundary at low H through Eq. (8). A value for the derivative $(dT_c/dH^2)_{H=0}$ that appears in Eq. (8) was taken from the calorimetric work of Johnson and Reese.[21] The value quoted there is $-9\times10^{-11}T_N$ K/G^2 which leads to the predicted values $q(n=3) = 6.8\times10^{-5}$ kG^{-2} and $q(n=2) = 8.1\times10^{-5}$ kG^{-2}. The ratio $Q = \omega_\perp/\omega_\parallel$ and the exponent ϕ are both universal, but the predicted values depend on the number n of bicritical spin components. The essential feature of ϕ is that it is larger than one, and the two predicted values $\phi(n=3) = 1.25$ and $\phi(n=2) = 1.18$ are not very different. For Q on the other hand, there is a considerable difference between the two values: $Q(n=3) = 2.51$ and $Q(n=2) = 1$.

Two different types of fits to Eqs. (9) were performed. First, the minimum possible number of adjustable parameters were used. All theoretically predicted values were inserted into Eqs. (9) and only T_b and $\omega_\perp$ were adjusted. Separate fits were tried for $n=3$ and $n=2$. In the second type, all five parameters, T_b, $\omega_\perp$, q, ϕ, and Q were adjusted simultaneously. For all fits, 18 points were used: ten points of the AF-P boundary and eight points of the C-P boundary. The best parameters were determined by minimizing the sum of the square deviations of H^2. The variance $\sigma^2(H^2) = (N-\nu)^{-1}\sum_i (\delta H_i^2)^2$ was determined for all fits (N being the number of points fitted and ν the number of parameters adjusted). For the fit of the second type, the standard deviation of the best parameters were also evaluated.[35]

The first type of fits revealed that a quite good fit could be obtained with $n=2$, but large systematic deviations were present for $n=3$. The best curves for these two fits are shown in Fig. 7: solid line for $n=2$; and dashed line for $n=3$. For $n=2$, the best adjusted parameters were: $T_b = 3.940$ K and $\omega_\perp = 0.996\times10^4$ kG^2. The square root of the variance for the best $n=2$ curve was $\sigma(H^2) = 1.5$ kG^2.

The second type of fit yielded: $T_b = 3.9398 \pm 0.0012$ K; $\omega_\perp = (1.7\pm0.4)\times10^4$ kG^2; $q = (7.1\pm2.0)\times10^{-5}$ kG^{-2}; $\phi = 1.29\pm0.07$; $Q = 1.06\pm0.22$ and $\sigma(H^2) = 1.2$ kG^2. The uncertainties quoted correspond to one standard deviation. The best curve is almost indistinguishable from the solid line in Fig. 7. Both types of fits give $H_b = 44.22$ kG.

The results of both types of fits showed that the data are in good general agreement with the FNK theory. It is significant the fact that comparably good fits were possible with just two parameters adjusted, as well as with five. In both cases, the value of $\sigma(H^2)$ is about one half of the resolution for measuring H^2 (which for H near H_b amounts to $\simeq 2.6$ kG^2), indicating that this resolution was the main cause for the deviations from the best curve. For the fit with five adjusted parameters, the resulting value of ϕ is higher than one, and close to the two predicted values. The resulting value of q is in good agreement with the predictions of Eq. (8). The standard deviations for q and ϕ are comparable to the predicted differences $[q(n=2) - q(n=3)]$ and $[\phi(n=3) - \phi(n=2)]$, respectively. Thus, the results for q and ϕ are insufficiently precise for assigning a particular value of n to the bicritical point. However, the fit with five adjustable parameters yield a value for Q which is in good agreement with the choice $n=2$, but is irreconcilable with $n=3$.

The $n=2$ behavior is reasonable for $NiCl_2 \cdot 6H_2O$. Theoretically, $n=3$ implies a perfectly uniaxial anisotropy. Although $NiCl_2 \cdot 6H_2O$ presents the gross features of a uniaxial antiferromagnet, its anisotropy has a small (but not negligible in the context of the discussion of bicritical points) orthorhombic component. According to Date and Motokawa[20] (see Table II), the anisotropy in the basal plane amounts to 2 kG, which is approximately 25% of the uniaxial anisotropy field, and approximately 3% of the exchange field. Such a basal plane anisotropy is sufficiently large to make the C-P transition Ising-like, so that $n=2$ at the bicritical point. For example, in MnF_2 a uniaxial anisotropy field of magnitude of 1% of the exchange field is sufficient to make the transition at T_N Ising-like.[16]

V. CONCLUSIONS

Measurements of the phase diagram of $NiCl_2 \cdot 6H_2O$ gave the following values for the exchange and anisotropy fields, at $T=0$: $H_E = 77.4 \pm 0.9$ kG; and $H_A = 10.8\pm0.3$ kG. They also provided data suitable for comparison with two theoretical predictions: (i) the temperature dependence of the C-P critical fields for $T \ll T_N$; and (ii) the behavior of the phase boundaries near the bicritical point.

For $0.07T_N \leq T \leq 0.24T_N$ the C-P transition

fields, $H_c(T)$, obeyed a $T^{3/2}$ law, as predicted by Falk,[9] Anderson and Callen,[10] and Feder and Pytte.[11] A least-squares fit to the equation $H_c(T) = H_c(0) - AT^{\alpha}$ for this temperature interval, gave $\alpha = 1.53 \pm 0.045$. However, fits of data for $T > 0.25T_N$ yielded α higher than $\frac{3}{2}$. In particular, for $0.3T_N \leq T \leq 0.6T_N$, the critical fields followed approximately a $T^{5/2}$ law similar to that found by Rives *et al.*[3,4] in $MnCl_2 \cdot 4H_2O$ and $CoCl_2 \cdot 6H_2O$ for comparable reduced temperatures. This result indicates that, to test the recent spin-wave predictions for these materials,[12] measurements at lower temperatures are needed.

Near the bicritical point, the phase boundaries showed good agreement with the FNK theory. Values of ϕ, q, and Q were obtained from a least-squares fit. The values of q and ϕ agreed with the predicted values, although without the accuracy necessary to distinguish between the $n = 2$ and $n = 3$ behavior. The value obtained for Q, however, sharply indicated a $n = 2$ behavior.

The $n = 2$ behavior near the bicritical point is a consequence of the small orthorhombic component of the anisotropy detected by antiferromagnetic resonance experiments.[20] Such an orthorhombicity is sufficiently large to affect the phase boundaries near the bicritical point. However, the present data suggest that this orthorhombicity is not sufficiently strong to cause the T^2 dependence for the low-T C-P critical field $H_c(T)$, as predicted by Cieplak.[12]

ACKNOWLEDGMENTS

We wish to thank Dr. Y. Shapira of the Francis Bitter National Magnet Laboratory of MIT for many helpful discussions. This work was partially supported by a joint grant from CNPq (Brazil) and NSF, and also partially supported by FINEP (Brazil). We are indebted to Dr. F. P. Missell for a critical reading of the manuscript. One of the authors (N.F.O.J.) gratefully acknowledges the support received from the Fundacão de Amparo á Pesquisa do Estado de São Paulo (Brazil). The Francis Bitter National Magnet Laboratory is supported by NSF.

[1]Y. Shapira and S. Foner, Phys. Rev. B 1, 3083 (1970).
[2]K. W. Blazey, H. Rohrer and R. Webster, Phys. Rev. B 4, 2287 (1971).
[3]J. E. Rives and V. Benedict, Phys. Rev. B 12, 1908 (1975).
[4]J. E. Rives and S. N. Bathia, Phys. Rev. B 12, 1920 (1975).
[5]H. Rohrer, Phys. Rev. Lett. 34, 1638 (1975).
[6]A. R. King and H. Rohrer, AIP Conf. Proc. 29, 420 (1976).
[7]Y. Shapira and C. C. Becerra, Phys. Lett. A 57, 483 (1976).
[8]Y. Shapira and C. C. Becerra, Phys. Rev. B 16, 4920 (1977).
[9]H. Falk, Phys. Rev. 133, A1382 (1964).
[10]F. B. Anderson and H. B. Callen, Phys. Rev. 136, A1068 (1964).
[11]J. Feder and E. Pytte, Phys. Rev. 168, 640 (1968).
[12]M. Cieplak, Phys. Rev. B 15, 5310 (1977).
[13]M. E. Fisher and D. R. Nelson, Phys. Rev. Lett. 32, 1550 (1974).
[14]M. E. Fisher, Phys. Rev. Lett. 34, 1634 (1975).
[15]J. M. Kosterlitz, D. R. Nelson, and M. E. Fisher, Phys. Rev. B 13, 412 (1976).
[16]M. E. Fisher, AIP Conf. Proc. 24, 273 (1975).
[17]The first precise determination of the C-P boundary for $T \ll T_N$ was made in the easy plane antiferromagnet EuTe ($T_N = 9.8$ K), by N. F. Oliveira, Jr., S. Foner and Y. Shapira, Phys. Lett. A 33, 153 (1970) [see also N. F. Oliveira, Jr., S. Foner, Y. Shapira, and T. B. Reed, Phys. Rev. B 5, 2634 (1972)]. In this material, the existence of a weaker ferromagnetic interaction, competing with a stronger antiferromagnetic interaction, lowers considerably the value of $H_c(0)$. The C-P boundary showed a $T^{3/2}$ behavior for $2 < T < 4.2$ K, but deviations were found for $T < 2$ K. It is not clear, however, whether the existent calculations apply to this case.
[18]N. F. Oliveira, Jr., A. Paduan Filho, and S. R. Salinas, AIP Conf. Proc. 29, 463 (1976); Phys. Lett. A 55, 293 (1975).
[19]R. Kleinberg, J. Appl. Phys. 38, 1453 (1967); J. Chem. Phys. 50, 5690 (1969).
[20]M. Date and M. Motokawa, J. Phys. Soc. Jpn. 22, 165 (1967).
[21]W. L. Johnson and W. Reese, Phys. Rev. B 5, 1355 (1970).
[22]A. I. Hamburger and S. A. Friedberg, Physica 69, 67 (1973).
[23]F. Keffer and H. Chow, Phys. Rev. Lett. 31, 1061 (1973).
[24]P. Pfeuty, D. Jasnow, and M. E. Fisher, Phys. Rev. B 10, 2088 (1974).
[25]P. Groth, Chem. Kryst. 1, 247 (1906).
[26]N. F. Oliveira, Jr., and C. J. A. Quadros, J. Phys. E 2, 967 (1969).
[27]Such a correction can also be affected by the presence of intense magnetic fields as pointed out by H. H. Sample and L. G. Rubin, Crogenics 18, 223 (1978).
[28]Manufactured by MKS Instruments Inc., 23 Third Ave., Burlington, Mass.
[29]L. G. Rubin and W. N. Lawless, Rev. Sci. Instrum. 42, 571 (1971).
[30]E. Maxwell, Rev. Sci. Instrum. 36, 553 (1965).
[31]R. M. Bozorth, *Ferromagnetism*, (Princeton, 1961), p. 849.
[32]T. Haseda, H. Kobayashi, and M. Date, J. Phys. Soc. Jpn. 14, 1724 (1959).
[33]I. Kimura, J. Phys. Soc. Jpn. 37, 946 (1974).
[34]T. Iwashita and N. Uryu, J. Phys. Soc. Jpn. 39, 58 (1975).
[35]A discussion about a least-squares fit to an arbitrary

function and error determination can be found in P. R. Bevington, *Data Reduction and Error Analysis for the Physical Sciences* (McGraw Hill, New York, 1969). A detailed description of the evaluation of standard deviations in a similar situation can be found in Y. Shapira and N. F. Oliveira, Jr., Phys. Rev. B 17, 4432 (1978).

[36]G. K. Chepurnykh, Fiz. Tverd. Tela. 10, 1917 (1968) [Sov. Phys. Solid State 10, 1517 (1968)].

[37]H. Rohrer and H. Thomas, J. Appl. Phys. 40, 1025 (1969).

[38]In a short note, A. Nakanishi, K. Okuda and M. Date, J. Phys. Soc. Jpn. 32, 282 (1972), published torque measurements showing that the easy axis of $NiCl_2 \cdot 6H_2O$ rotates by a few degrees in the a-c plane, as a function of temperature, above and below T_N. This rotation affects the alignment between $\vec{H}$ and the easy axis. However, from the published figure, we estimated that the total angular displacement in the whole temperature interval of interest for the interpretation of our data near T_b is $\lesssim 0.05°$. The effects of such small displacement in our results are negligble.